engineering proceedings

MDPI

Proceeding Paper

Temperature-Dependent Dielectric Studies of Copper-and-Magnesium-Doped Zinc Aluminate: Implications for Electrical Behaviour †

Yasmin Jamil, Gracie. P. Jeyakumar and Geetha Deivasigamani *

Department of Applied Sciences and Humanities, Madras Institute of Technology, Anna University, Chennai 600044, India

* Correspondence: geetha@mitindia.edu

† Presented at the 4th International Electronic Conference on Applied Sciences, 27 October–10 November 2023; Available online: https://asec2023.sciforum.net/.

Abstract: Copper (Cu^{2+})-and-magnesium (Mg^{2+})-doped Zinc aluminate $ZnAl_2O_4$ is a promising material with diverse applications in electronic and energy storage devices. In this study, the synthesis of $Zn_{0.9}M_xAl_2O_4$ (M = Cu^{2+} and Mg^{2+}; x = 0.00 and 0.10) was conducted via the sol–gel combined combustion technique. The structural, spectral, optical and dielectric parameters of the synthesized spinel aluminates were analysed to explore the substitution effect of Cu^{2+} and Mg^{2+} content. The formation and crystallinity analyses of the single-phase cubic spinel structure in the synthesized spinel aluminates were confirmed using XRD patterns. The lattice parameter and grain size were ascertained from the XRD data. The crystallite size of Cu^{2+} and Mg^{2+} substituted into $ZnAl_2O_4$ using Scherrer's formula was found to be around 22 nm. The spinel structure formations in the prepared spinel aluminates were ascertained through an FT-IR study. The UV-Vis spectra exhibited a broad absorption band in the UV-Vis region, indicating the presence of electronic transitions. The band gap energy of the prepared aluminates was estimated from the absorption edge, with values varying between 2.90 eV and 3.03 eV, revealing its suitability for optoelectronic applications. Measurement of the dielectric parameters was performed in the frequency range of 100 Hz to 20 MHz at temperatures ranging from 30 °C to 250 °C. The dielectric constant (ε') and dielectric loss (ε'') were determined as a function of frequency at different temperatures. The results showed that the dielectric constant decreased with increasing frequency for all the observed temperatures, while the dielectric loss exhibited a peak at a specific temperature. The conductivity results indicate that the conduction mechanism occurred due to polaron hopping. The Arrhenius relation was adopted to calculate the activation energies E_a for all the samples, and the values were between 0.70 eV and 0.38 eV. The obtained results were discussed and interpreted. These findings contribute to our understanding of the electrical behaviour of doped zinc aluminate materials and their useful applications in different electronic and energy systems.

Keywords: combustion method; band gap; Maxwell–Wagner; Ac conductivity

Citation: Jamil, Y.; Jeyakumar, G.P.; Deivasigamani, G. Temperature-Dependent Dielectric Studies of Copper-and-Magnesium-Doped Zinc Aluminate: Implications for Electrical Behaviour. *Eng. Proc.* **2023**, *56*, 213. https://doi.org/10.3390/ASEC2023-16270

Academic Editor: Manoj Gupta

Published: 15 November 2023

1. Introduction

Spinel $ZnAl_2O_4$ represents a class of fascinating materials that exhibit intriguing and versatile applications due to their unique crystal structure and composition. The semiconductor $ZnAl_2O_4$ has fascinating characteristics that make it suitable for broad technological applications like sensors, photocatalysts, microwave devices, ceramic pigments and microelectronics. Also, due to its remarkable properties, like a high melting point and a large surface area, it is widely studied for high-temperature fuel cells, dielectric materials and other optoelectronic applications [1,2]. The substitution or doping of transition metal ions into the aluminate system results in the enhancement of its optical and electrical properties. The aim of the current research is: (i) to improve the properties of zinc aluminate by

bringing down the dimensions to nanosize and (ii) to observe the effects of substitution on its structural, optical and dielectric properties. Earlier studies on nanocrystalline $ZnAl_2O_4$ have reported a low dielectric constant, better conductivity and enhanced optical properties [3]. Various synthesis routes have been adopted to synthesize spinel aluminates, like the cost-effective sol–gel auto combustion method, co precipitation method, mixed oxide method and microwave method. Out of all these methods, the sol–gel auto combustion method is the most reliable and cost-effective method to synthesize spinel aluminates. Hence, a simple sol–gel auto combustion method was adopted to synthesize single-phase $Zn_{1-x}Cu_xAl_2O_4$ and $Zn_{1-x}Mg_xAl_2O_4$ (x = 0.0 and 0.1). We discuss the effects of Cu and Mg substitution on $ZnAl_2O_4$, and their structural, optical and dielectric properties are discussed in detail.

2. Materials and Methods

Nitrate precursors in the form of zinc $Zn(NO_3)_2.6H_2O$, aluminium $Al(NO_3)_2.9H_2O$, cupric $Cu(NO_3)_2.3H_2O$ and magnesium Mg $(NO_3)_2.6H_2O$ were used for the preparation of spinel aluminates. Citric acid monohydrate ($C_6H_8O_7.H_2O$) as a chelating agent, distilled water H_2O as a solvent and ammonia solution to balance the pH at 9 were used. $Zn(NO_3)_2.6H_2O$, $Al(NO_3)_2.9H_2O$ and $C_6H_8O_7.H_2O$ in a stoichiometric ratio of 1:2:2 were dissolved in sufficient amount of distilled water, and the solution was magnetically stirred for 2 h at room temperature. Ammonia solution was added dropwise until the desired pH was reached. The temperature was then gradually increased after 2 h for gelation. The obtained gel was combusted at 100 °C and the powders were calcined at 800 °C for 3 h. For Cu- and Mg-substituted samples, the same procedure was adopted by adding the Cu and Mg derivatives into the solution. The samples were then named ZnAl, ZnAl:Cu and ZnAl:Mg. The obtained aluminate powders were utilized for further characterization.

The phase and crystalline structure were characterized by the X-ray diffraction technique (XRD: D8 Advance Bruker AXS, Berlin, Germany). Functional groups in the 400–4000 cm^{-1} spectral range were used to compute the designated transmittance bands using Fourier transform infrared spectroscopy (FTIR—Shimadzu). The optical spectral analysis was carried out via UV-DRS spectroscopy (SHIMADZU UV-1800, Kyoto, Japan). Broadband dielectric spectroscopy BDS (NOVOCONTROL) was used to record the dielectric parameters in the frequency range of 100 Hz–20 MHz at temperatures ranging from room temperature to 250 °C.

3. Results and Discussion

3.1. Structural Properties—XRD

The diffraction patterns of ZnAl, ZnAl:Cu and ZnAl:Mg, shown in Figure 1, were estimated using the X-ray diffraction method. The XRD patterns ensured the formation of the uni-phase spinel cubic structure of the prepared aluminates. The obtained patterns were indexed with Miller indices of (111), (220), (311), (400), (331), (422), (511), (440), (620) and (533) associated with the various planes, and the observed results were in correlation with JCPDS card No: 05-0669 and earlier reported literature [4].

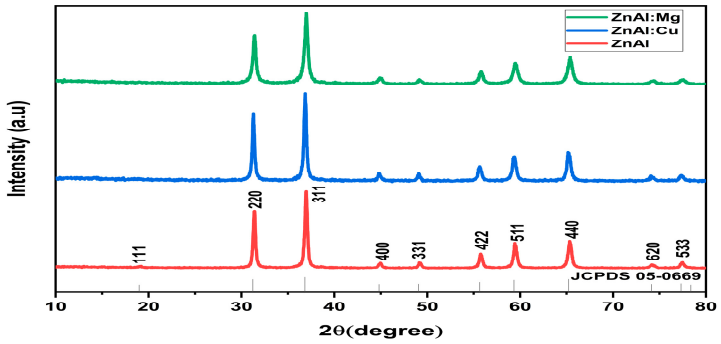

Figure 1. XRD patterns of ZnAl, ZnAl:Cu and ZnAl:Mg.

The lattice parameter (a) was obtained for the high intense peak (311) using the Nelson-Riley relation:

$$f(\theta) = \frac{1}{2}\left(\frac{cos^2\theta}{sin\theta} + \frac{cos^2\theta}{\theta}\right) \quad (1)$$

where θ is the angle of diffraction. The lattice parameters of ZnAl:Cu and ZnAl:Mg are lesser than the parent ZnAl, which may be due to the ionic radii of the substituted cation reordering with the cubic spinel phase. The volume of the unit cell was calculated using $V = a^3$, and the crystallite size (D) was calculated by employing Scherrer's formula, which is given by

$$D = \frac{k\lambda}{\beta cos\theta} \quad (2)$$

where k is shape factor whose value is 0.9, λ is the wavelength of the Cu-Kα source, β is the full width half maximum (FWHM) and θ is the diffraction angle. The average crystallite size and structural parameters calculated from the XRD patterns are shown in Table 1.

Table 1. Structural parameters of ZnAl, ZnAl:Cu and ZnAl:Mg.

Samples	Crystallite Size D (nm)	Lattice Parameter a (A°)	Dislocation Density δ	Volume of the Unit Cell $V = a^3$ (A°)
ZnAl	22.818	8.0815	1.9205	527.69
ZnAl:Cu	23.048	8.0564	1.8823	523.54
ZnAl:Mg	22.920	8.0575	1.9034	523.56

3.2. FT-IR Analysis

The FT-IR patters of ZnAl, ZnAl:Cu and ZnAl:Mg are shown in Figure 2. The assurance of the spinel structure was confirmed from the transmittance bands present in the fingerprint region of 450 cm^{-1} to 790 cm^{-1}. The occurrence of transmittance bands at 661.53 cm^{-1} is associated with the vibration of Zn-O, the band at 554.49 cm^{-1} is associated with the vibration of Al-O, and the band at 496.63 cm^{-1} can be associated with the vibration of Zn-O-Al at tetrahedral and octahedral sites, respectively. The aluminate samples also contain another transmittance bands around 2354.27 cm^{-1} and 3437.87 cm^{-1} which are associated with the CO_2 bands and -O-H stretching band, respectively. The other bands at 1627 cm^{-1} and 1408 cm^{-1} are associated with the symmetric and asymmetric vibrations of C-H [5]. The intensity of the transmittance bands gets broader and shorter due to substitution of Cu and Mg in the zinc site and due to the ionic radii of the substitution ion.

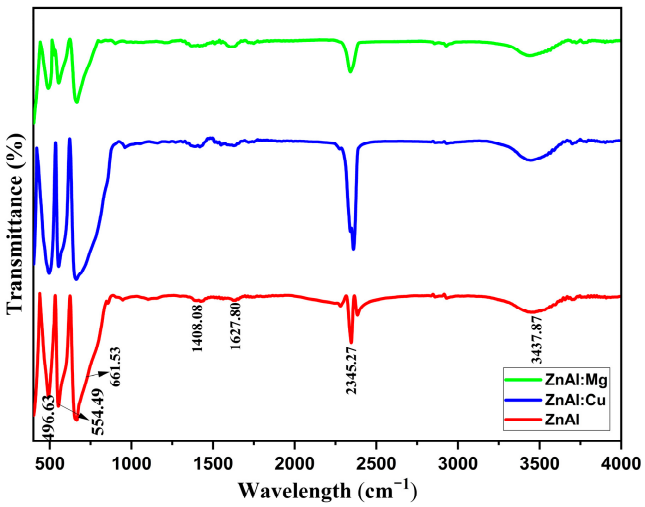

Figure 2. FT-IR spectra of ZnAl, ZnAl:Cu and ZnAl:Mg.

3.3. UV-DRS Analysis

The optical energy band gaps of ZnAl, ZnAl:Cu and ZnAl:Mg recorded in the range of 200–800 nm using the UV-DRS technique are shown in Figure 3. Strong absorption peaks for all the aluminates are observed in the visible region of the spectra. The band gap energy was calculated using the Tauc's relation, given by

$$(\alpha h\nu)^n = A(h\nu - E_g) \quad (3)$$

where α is the absorption coefficient, $h\nu$ is the photon energy, A is a constant depending on the type of transition and n is the coefficient of allowed transitions. For the direct band gap, $n = 1/2$, and for the indirect band, $n = 2$. By finding the intercept on the $h\nu$ axis and extrapolating the plot $(\alpha h\nu) = 0$, the band gap can be estimated [6,7]. The optical direct band gap energy values of ZnAl, ZnAl:Cu and ZnAl:Mg were 3.03 eV, 2.94 eV and 2.90 eV, respectively. As seen from Figure 3, the band gap energy of Cu and Mg doped aluminates was found to decrease compared to the parent sample. This may be due to the quantum confinement effect owing to the small crystallite size of the prepared aluminates [3].

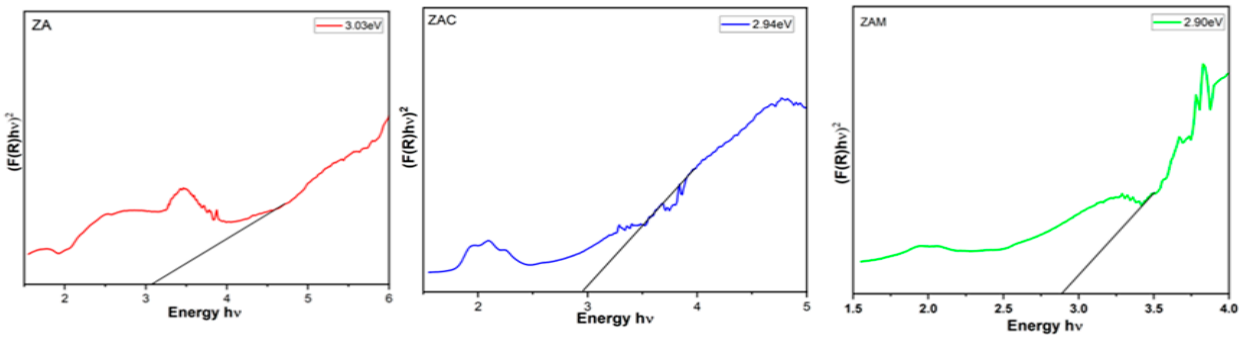

Figure 3. Tauc's plots of ZnAl, ZnAl:Cu and ZnAl:Mg.

3.4. Temperature-Dependent Dielectric Parameters

3.4.1. Dielectric Studies: Dielectric Constant ε', Tangent Loss tan δ and AC Conductivity σ_{ac}

The real and imaginary parts of the dielectric constant ε' are expressed in terms of complex permittivity, as given below:

$$\varepsilon'(\omega) = \varepsilon_\infty + \frac{\varepsilon_s - \varepsilon_\infty}{1 + \omega^2\tau^2} \quad (4)$$

$$\varepsilon''(\omega) = \varepsilon_s - \varepsilon_\infty + \frac{\omega\tau}{1 + \omega^2\tau^2} \quad (5)$$

where ε_∞ is the permittivity at a higher frequency limit, ε_s is the static low-frequency permittivity and τ is the characteristic relaxation time of the medium. The above two equations are known as Debye equations. Equation (4) gives a clear understanding of the decline in the dielectric constant ε' with an increase in frequency. Figure 4A–C represent the dielectric constant ε' of ZnAl, ZnAl:Cu and ZnAl:Mg as a function of frequency ranging from 100 Hz to 20 MHz at temperatures of 303–523 K. It can be observed that the dielectric constant is very high in a lower frequency domain, and as it approaches a higher frequency, the dielectric constant ε' achieves a minimum value or becomes constant. This dispersive nature of the dielectric constant ε' can be explained by Maxwell–Wagner-type interfacial polarization, as suggested by Koop's model, which states that in low-frequency regions, the charge carriers have a tendency to follow the applied electric field, whereas in high-frequency regions, the charge carriers cause the applied electric field to lag, which results in a decline in the dielectric constant ε' [8,9]. It is known that the grain boundaries are primarily composed of O_2 and non-stoichiometric dangling bonds, which function as electron traps within the system. On applying an electric field, the mobile electrons

move towards the grain boundary through the conductive path's grains, facilitated by the dangling bonds present. Owing to high resistance at the grain boundary, the mobile electrons gather there, resulting in elevated dielectric values at lower frequencies, whereas as the applied field increases, a significant portion of the electrons lose their capability to respond to the electric field applied and consequently change direction more rapidly, making it difficult to reach the grain boundaries, and the dielectric constant ε' substantially decreases in higher-frequency regions [10,11]. We can also see that as temperature increases, the dielectric constant decreases ε' at low frequencies for all the temperatures as a result of thermal activation and accommodates more charges at grain boundaries. However, it reaches a minimum value at higher frequencies for all the observed temperatures. The composition dependence of the dielectric constant can be explained by the electron exchange between Al^{2+} and Al^{3+} octahedral sites and the polaron hopping of electrons [11]. When Cu and Mg are substituted into the parent material at the Zn site, the dielectric constant ε' decreases because Cu and Mg have a higher probability of accommodating B-site ions. As a result of this, there is a reduction in the concentration of aluminium ions at octahedral sites, which ruptures the charge transfer between Al^{2+} and Al^{3+}, and this affects the polarization mechanism.

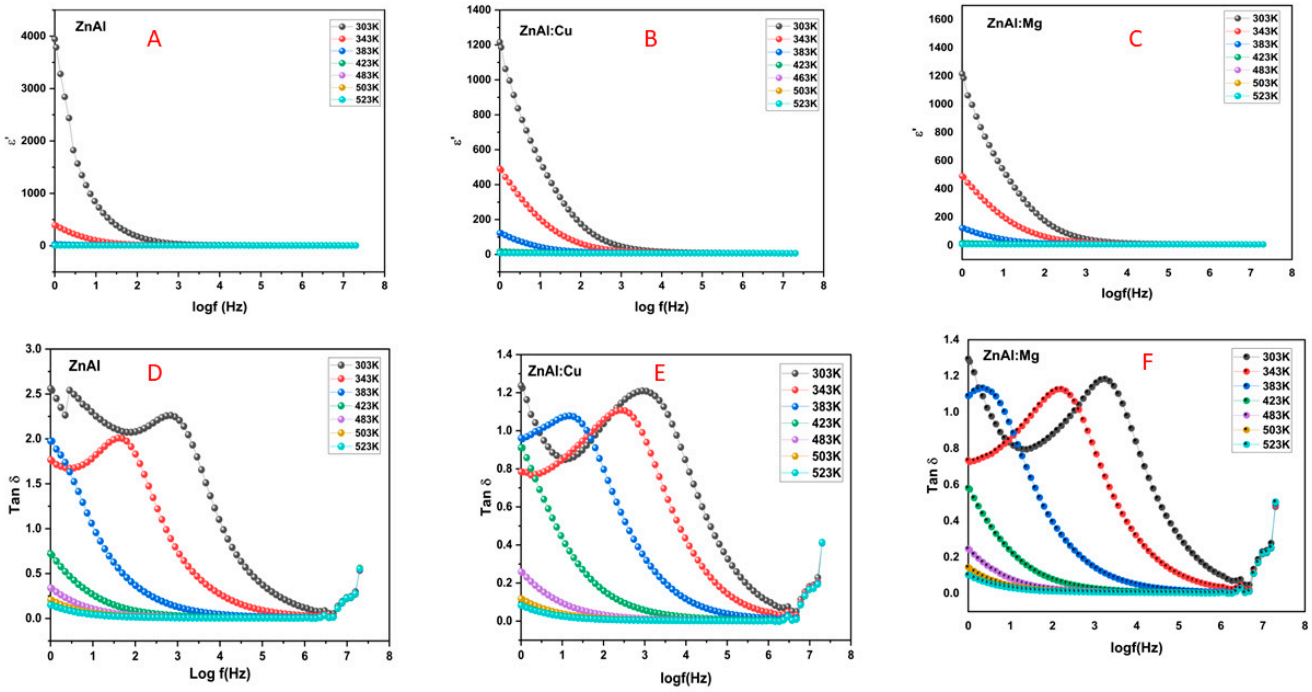

Figure 4. Dielectric constant ε' (**A**–**C**) and tangent loss tan δ (**D**–**F**) of ZnAl, ZnAl:Cu and ZnAl:Mg vs. frequency at several temperatures.

Figure 4D–F represent the tangent loss tan δ of ZnAl, ZnAl:Cu and ZnAl:Mg as a function of frequency ranging from 100 Hz to 20 MHz at temperatures of 303–523 K. The tangent loss is given by

$$\tan \delta = \frac{\varepsilon''}{\varepsilon'} \quad (6)$$

In the lower-frequency region, tan δ increases, and as frequency increases, the loss decreases. Each sample shows some extraordinary behaviour in the lower-frequency region at specific temperatures. The presence of a relaxation peak in the curve in the lower-frequency region indicates that the dielectric constant contribution is large due to the variation in tan δ and due to the accumulation of charge carriers at low temperatures and frequencies [3,9]. The hopping of electrons at low frequencies needs sufficient energy due to the resistive nature of grains and grain boundaries, which results in a high value of tan

δ. A higher frequency results in minimum electron hopping because the resistive nature of grain boundaries decreases and energy consumption is less. Also, there are sometimes additional losses which may be due to disorders in the crystal system and imperfections. As the temperature decreases, the values of tangent loss decrease, and these results are in line with those of previous studies. The tangent loss has the lowest value for the Cu- and Mg-substituted samples compared with the parent sample.

3.4.2. Ac Conductivity

The ac conductivity σ_{ac} of ZnAl, ZnAl:Cu and ZnAl:Mg as a function of frequency ranging from 100 Hz to 20 MHz at temperatures of 303–523 K is displayed in Figure 5. From the ac conductivity plot, it is seen that as frequency increases, the conductivity also increases at all the given temperatures for all the samples, and the values of conductivity are larger in higher-frequency regions due to the polaron hopping present in sample [8,9]. The frequency- and temperature-dependent conductivity are closely associated with the universal Jonscher's power law given by the relation

$$\sigma_t = \sigma_{dc} + A\omega^n \tag{7}$$

where σ_t is the total conductivity, σ_{dc} is the dc conductivity and temperature-dependent conductivity, ω is the angular frequency $\omega = 2\pi f$, A is coefficient and n is the frequency exponent dependent on temperature. Jonscher's power law is obtained by plotting $\ln(\sigma_{ac})$ as a function of logarithmic frequency, as shown in Figure 5.

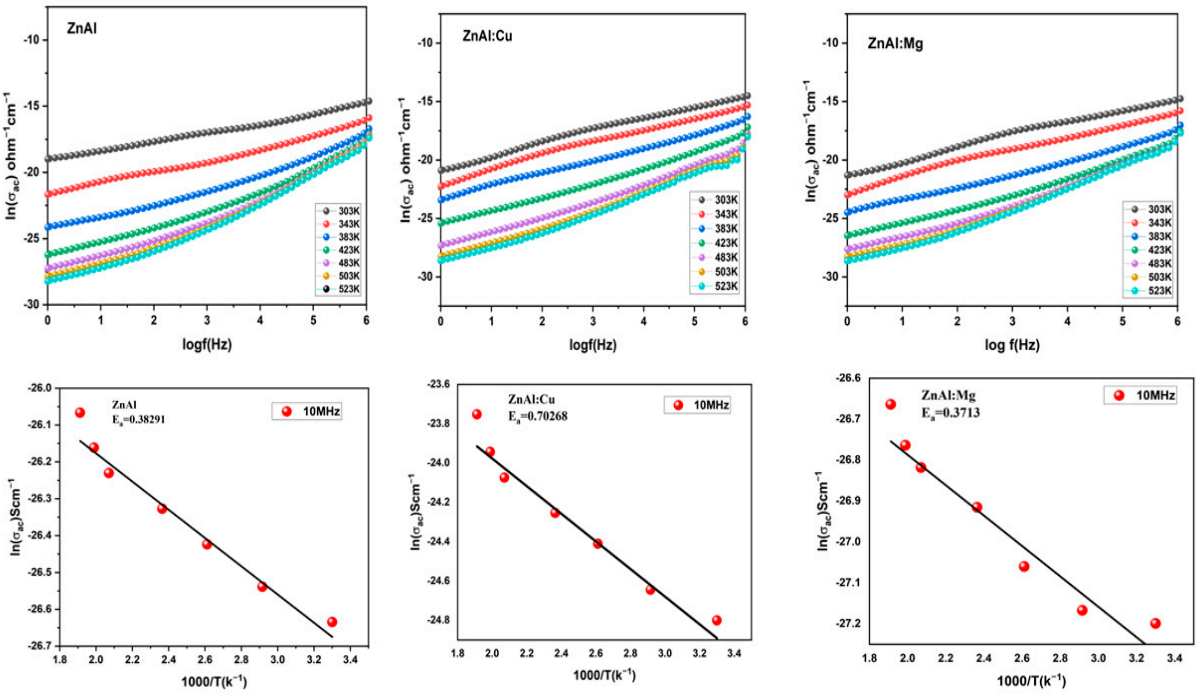

Figure 5. AC conductivity plots of of ZnAl, ZnAl:Cu and ZnAl:Mg at various temperatures and Arrhenius plots of ZnAl, ZnAl:Cu and ZnAl:Mg at 10 MHz.

The relation between ac conductivity σ_{ac}, real dielectric constant ε, frequency and dielectric loss can be expressed as

$$\sigma_{ac} = \varepsilon' \varepsilon_0 \omega \tan\delta \tag{8}$$

The dielectric structure of spinel systems consists of two layers, i.e., conducting grains and non-conducting grain boundaries. On applying the field, the long-range inter-well hopping of holes between Al^{2+} and Al^{3+} sites located near defect-potential wells or short

range intra-well hopping within one defect-potential well may occur [3,12]. The dc part of the total conductivity contributes to inter-well hopping, while ac conductivity contributes to intra-well hopping. Hence, a gradual increase in ac conductivity with frequency is observed. Using the temperature-dependent ac and dc conductivity, the activation energy can be calculated using the Arrhenius relation given by

$$\sigma_{ac} = \sigma_o exp \frac{-E_a}{k_B T} \quad (9)$$

where σ_o is the pre-exponential factor Boltzmann's constant with temperature ($k_B T$), and E_a is the activation energy of the sample. A plot of log(σ_{ac}) vs. 1000/T is shown in Figure 5. The activation energies of ZnAl, ZnAl:Cu and ZnAl:Mg for 10 MHz were found to vary between 0.70 eV and 0.38 eV.

4. Conclusions

A simple sol–gel combustion method was used to prepare spinel Cu- and Mg-substituted zinc aluminates. XRD patterns confirmed the single-phase formation of synthesized aluminates with an average crystallite size varying between 22.6 nm and 23.05 nm. The characteristic transmittance bands in the fingerprint region confirms the spinel structure of the aluminates. The optical spectra indicated a decrease in the band gap of the aluminates, and the values were found to be 3.03 eV, 2.90 eV and 2.94 eV for ZnAl, ZnAl:Cu and ZnAl:Mg, respectively. The dielectric constant ε' and tangent loss tan δ values of the synthesized zinc aluminates decreased substantially at higher frequencies for all the observed temperatures, obeying Maxwell–Wagner interfacial polarization. The AC conductivity σ_{ac} spectra of the synthesized zinc aluminates as a function of frequency at several temperatures was investigated, and the conductivity increased as the frequency increased. The conductivity mechanism was discussed in detail based on grain and grain boundary contribution and the hopping mechanism. The activation energies of the synthesized zinc aluminates were calculated using the Arrhenius relation, and the values were between 0.70 eV and 0.38 eV. The activation energy E_a of ZnAl:Cu was found to be the highest. From the observed results, it can be propounded that these synthesized aluminates could be used for high-frequency applications and memory-based storage devices.

Author Contributions: Conceptualization, Y.J.; methodology, Y.J.; software, Y.J.; validation, Y.J., G.P.J. and G.D.; formal analysis, Y.J.; investigation, Y.J.; data curation, Y.J. and G.P.J.; writing—original draft preparation, Y.J.; writing—review and editing, Y.J.; visualization, G.D. and Y.J.; supervision, G.D.; project administration, G.D. All authors have read and agreed to the published version of the manuscript.

Funding: This research was funded by the Anna Centenary Research Fellowship (ACRF), Anna university, with Ref No. CFR/ACRF-2022/AR1.

Institutional Review Board Statement: Not applicable.

Informed Consent Statement: Not applicable.

Data Availability Statement: Data are contained within the article.

Acknowledgments: Author Yasmin J gratefully acknowledges Anna University, Chennai, for providing an ACRF Fellowship to carry out this research work.

Conflicts of Interest: The authors declare no conflicts of interest.

References

1. Srinatha, N.; Satyanarayana, R.; Suriyamurthy, N.; Rudresh Kumar, K.J.; Suresh Kumar, M.R.; Madhu, A.; Angadi, B. New fuel governed combustion synthesis and improved luminescence in nanocrystalline Cr^{3+} doped $ZnAl_2O_4$ particles. *Results Opt.* **2022**, *8*, 100242. [CrossRef]
2. Jamil, Y.; Jeyakumar, G.P.; Deivasigamani, G. Investigation of Transition Metal Ions Cu^{2+} and Mg^{2+} Doped Zinc Aluminate ($ZnAl_2O_4$) and Their Structural, Spectral, Optical, and Dielectric Study for High-Frequency Applications. *Mater. Proc.* **2023**, *14*, 2.

3. Muhammad, E.; Jamal, A.; Kumar, S.; Anantharaman, M.R. On structural, optical and dielectric properties of zinc aluminate nanoparticles. *Bull. Mater. Sci.* **2011**, *34*, 251–259.
4. Han, M.; Wang, Z.; Xu, Y.; Wu, R.; Jiao, S.; Chen, Y.; Feng, S. Physical properties of $MgAl_2O_4$, $CoAl_2O_4$, $NiAl_2O_4$, $CuAl_2O_4$, and $ZnAl_2O_4$ spinels synthesized by a solution combustion method. *Mater. Chem. Phys.* **2018**, *215*, 251–258. [CrossRef]
5. Lu, Q.; Wei, Z.; Wu, X.; Huang, S.; Ding, M.; Ma, J. Electronic structure and optical properties of spinel structure $Zn_{1-x}Ni_xAl_2O_4$ nanopowders synthesized by sol–gel method. *Chem. Phys. Lett.* **2021**, *772*, 138582. [CrossRef]
6. Priya, A.S.; Geetha, D. Impact of (Zr, Cu) ion substitution on the optical, dielectric, and impedance behavior of $BiFeO_3$. *Braz. J. Phy.* **2021**, *51*, 40–46. [CrossRef]
7. Elakkiya, V.; Agarwal, Y.; Sumathi, S. Photocatalytic activity of divalent ion (copper, zinc and magnesium) doped $NiAl_2O_4$. *Solid State Sci.* **2018**, *82*, 92–98. [CrossRef]
8. Rajamoorthy, M.; Geetha, D.; Sathiya Priya, A. Synthesis of Cobalt-Doped $Bi_{12}NiO_{19}$: Structural, Morphological, Dielectric and Magnetic Properties. *Arab. J. Sci. Eng.* **2021**, *46*, 737–744. [CrossRef]
9. Saleem, M.; Varshney, D. Influence of transition metal Cr^{2+} doping on structural, electrical and optical properties of Mg-Zn aluminates. *J. Alloys Compd.* **2017**, *708*, 397–403. [CrossRef]
10. Priya, A.S.; Geetha, D. Studies on the multiferroic properties and impedance analysis of (La, Cu) $BiFeO_3$ prepared by sol-gel method. *Ferroelectrics* **2021**, *573*, 104–116. [CrossRef]
11. Samkaria, R.; Sharma, V. Effect of rare earth yttrium substitution on the structural, dielectric and electrical properties of nanosized nickel aluminate. *Solid State Mater. Adv. Technol.* **2013**, *178*, 1410–1415. [CrossRef]
12. Mahmood, A.; Maqsood, A. Temperature and frequency-dependent electrical transport studies of manganese-doped zinc ferrite nanoparticles. *Mater. Sci. Eng. B* **2023**, *296*, 116615. [CrossRef]